

See discussions, stats, and author profiles for this publication at: <https://www.researchgate.net/publication/300576518>

Active Vision Speed Estimation from Optical Flow

Conference Paper · June 2014

DOI: 10.1007/978-3-662-43645-5_18

CITATIONS

2

READS

1,612

2 authors:



Sotirios Diamantas

Tarleton State University

17 PUBLICATIONS 82 CITATIONS

[SEE PROFILE](#)



Raj Dasgupta

University of Nebraska at Omaha

140 PUBLICATIONS 1,373 CITATIONS

[SEE PROFILE](#)

Some of the authors of this publication are also working on these related projects:



Improved Reward Estimation for Efficient Robot Navigation Using Inverse Reinforcement Learning [View project](#)



Real-Time Robot Path Planning Around Complex Obstacle Patterns through Learning and Transferring Options [View project](#)

Active Vision Speed Estimation From Optical Flow

Sotirios Ch. Diamantas and Prithviraj Dasgupta

C-MANTIC Lab, Department of Computer Science
University of Nebraska, Omaha. Omaha, NE 68182, USA
{sdiamantas,pdasgupta}@unomaha.edu
<http://cmantic.unomhaha.edu>

Abstract. In this research, we address an important problem in mobile robotics - how to estimate the speed of a moving robot or vehicle using optical flow obtained from a series of images of the moving robot captured by a camera. Our method generalizes several restrictions and assumptions that have been used previously to solve this problem - we use an uncalibrated camera, we do not use any reference points on the ground or on the image, and we do not make any assumptions on the height of the moving target. The only known parameter is the camera distance from the ground. In our method we exploit the optical flow patterns generated by varying the camera focal length in order to pinpoint the principal point on the image plane and project the camera height on the image plane. This height is then used to estimate the speed of the target.

Keywords: Speed estimation, principal point estimation, optical flow, active vision

1 Introduction

In this paper we describe our research on estimating a moving vehicle's speed using optical flow vectors. A few decades ago and up to date most of the effort on speed estimation has been focused on using Time-of-Flight (TOF) sensors. Since the advent of visual perception sensors a significant number of research has been devoted on estimating speed using cameras. One main reason is that cameras provide an efficient yet inexpensive means for speed estimation. Furthermore, the use of computational techniques has advanced the field by providing satisfactory estimations. Moreover, cameras are also used, for example, in road traffic for purposes beyond speed estimation such as monitoring, plate recognition, and vehicle tracking.

In this research we make two contributions. The first contribution is that we estimate the principal point of an uncalibrated camera by exploiting the inherent properties of today's modern digital cameras. In particular, we make use of active vision by varying the focal length of the camera, that is the optical zoom, with the view to estimate the point in the image plane that is invariant

to rotation and lens translation. In every lens there is an imaginary optical axis that is coming out of its center. The projection of the optical axis onto the image plane is the principal point. However, the optical axis of the lens is almost never aligned with the center of the image sensor. For this reason, in order to estimate parameters such as the principal point, most of the methods employed rely upon camera calibration techniques. In our approach we have used an uncalibrated camera to infer the principal point by varying the focal length of the camera; a technique that can be used in real-time on most robotic systems.

The second contribution is that we estimate the speed of a moving vehicle, namely a *Corobot* mobile robot with minimal assumptions. We make no use of artificial marks on the ground nor any other assumptions such as the distance between two points or a reference object in the image plane. In addition, the distance between the camera and the moving object need not be known. The only known parameter that we employ as a reference point for estimating the speed of the vehicle is the height of the visual sensor from the ground which is available or can be calculated in most vision-based systems. Yet, the visual sensor in our method is placed parallel to the ground; a case which holds for most robotic and other systems. The proposed method can easily be applied to several robotic tasks such as navigation, localization, and height estimation.

The following section provides a literature review on vehicle speed estimation as well as the mathematics that underlie optical flow. In Section 3 the methodology of applying optical flow for principal point and speed estimation is described. In Section 4 the results of our method are presented and finally Section 5 epitomizes the paper with a section on the conclusions drawn from this research as well as the prospects for future work.

2 Background Work

Optical flow, that is the rate of change of image motion in the retina or a visual sensor, is extracted from the apparent motion of an agent be it natural or artificial. Although motion is an inherent property of optical flow, there is not a large number of works that employ optical flow for speed estimation. In [1] the authors present an optical flow method for speed estimation using a calibrated camera. A method of speed estimation that does not rely on a calibrated camera but instead makes assumptions drawn from a distribution about the mean height, width, and length of the vehicle is presented in [2].

In [3] the authors present a method similar to the one followed in our research for speed estimation. However, they know in advance the height of the moving vehicle. In particular, they use a measurement tape to infer the heights of the vehicle. An optical flow method for velocity estimation for Micro Aerial Vehicles (MAVs) is presented in [4]. In that work, the authors use an FPGA platform in order to extract the optical flow field. Their research is suitable for embedded systems since most of the calculations take place on an FPGA. A method for speed estimation using a known ground distance along the road axis is presented in [5]. A velocity estimation for a blimp using a non-optical but air flow sensor

appears in [6] where particle filtering and a probabilistic model are employed. In [7] the authors present an embedded system for vehicle speed estimation. An RF-based method for speed estimation appears in [8]. In [9] the authors make use of magnetic signatures induced by vehicles to estimate the speed of vehicles in highways.

The problem of estimating the heights of objects by means of the focus of expansion (FOE) is addressed in [10]. In that work the authors use the cross ratio of a known object's height in the image plane in order to estimate other object's heights in the same image. Reference objects are also used in the seminal work of [11]. A method for height estimation using a single image from an uncalibrated camera and a vanishing point is described in [12]. An active vision technique for zoom tracking by varying the focal length of the camera is presented in [13]. Our research in contrast to the afore-mentioned works can estimate the speed of a vehicle with an uncalibrated camera and with no reference objects in the image plane. Furthermore, our research, similarly to the work of [10], makes use of feature points. However, we exploit the focal length of the visual sensor to achieve near (pure) translation instead of the robot movement.

2.1 Mathematics of Optical Flow

This section describes the mathematics of optical flow algorithms, and in particular, the Lucas-Kanade (LK) algorithm [14] which has been employed in this research. Following are the equations needed for a 5×5 pixels window that results in a system of 25 linear equations that need to be solved (1). However, if the window is too small the *aperture problem* may be encountered where only one dimension of the motion of a pixel can be detected and not the two-dimensional. On the other hand, if the window is too large then the spatial coherence criterion may not be met.

$$\underbrace{\begin{bmatrix} I_x(p1) & I_y(p1) \\ I_x(p2) & I_y(p2) \\ \vdots & \vdots \\ I_x(p25) & I_y(p25) \end{bmatrix}}_{A=25 \times 2} \underbrace{\begin{bmatrix} u \\ v \end{bmatrix}}_{u=2 \times 1} = - \underbrace{\begin{bmatrix} I_t(p1) \\ I_t(p2) \\ \vdots \\ I_t(p25) \end{bmatrix}}_{b=25 \times 1} \quad (1)$$

The goal on the above system of linear equations is to minimize $\|A\mathbf{u} - b\|^2$ where $A\mathbf{u} = b$ is solved by employing least-squares minimization as in (2),

$$(A^T A)\mathbf{u} = A^T b \quad (2)$$

where $A^T A$, \mathbf{u} , and $A^T b$ are equal to (3),

$$\underbrace{\begin{bmatrix} \sum I_x^2 & \sum I_x I_y \\ \sum I_x I_y & \sum I_y^2 \end{bmatrix}}_{A^T A} \underbrace{\begin{bmatrix} u \\ v \end{bmatrix}}_{\mathbf{u}} = - \underbrace{\begin{bmatrix} \sum I_x I_t \\ \sum I_y I_t \end{bmatrix}}_{A^T b} \quad (3)$$

and the solution to the equation is given by (4)

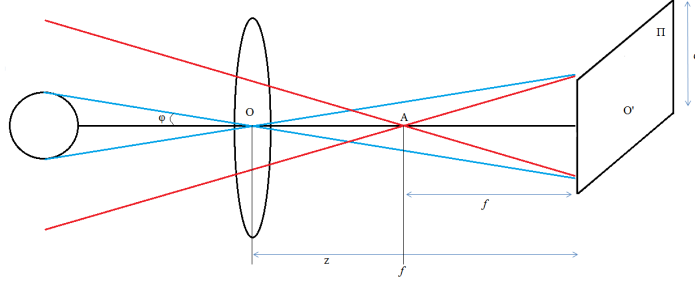


Fig. 1. Optical axis, O , of a lens and its projection onto the image plane, Π , that is, principal point, O' . In this figure a zoom lens is depicted with varying focal lengths between points OA . Zoom lens range is represented with z and lies within the points OA . Sensor's width is represented with d and ϕ is the angle between an object (e.g., ball) and the center of the lens.

$$\mathbf{u} = \begin{bmatrix} u \\ v \end{bmatrix} = (A^T A)^{-1} A^T b. \quad (4)$$

If $A^T A$ is invertible, i.e., no zero eigenvalues, it means it has full rank 2 and two large eigenvectors. This occurs in images where there is high texture in at least two directions. If the area that is tracked is an edge, then $A^T A$ becomes singular, that is (5),

$$\begin{bmatrix} \sum I_x^2 & \sum I_x I_y \\ \sum I_x I_y & \sum I_y^2 \end{bmatrix} \begin{bmatrix} -I_y \\ I_x \end{bmatrix} = \begin{bmatrix} 0 \\ 0 \end{bmatrix} \quad (5)$$

where $-I_y, I_x$ is an eigenvector with eigenvalue 0. If the area of interest is homogeneous then $A^T A \approx 0$, implying 0 eigenvalues. The pyramidal approach of the LK algorithm overcomes the local information problem at the top layer by tracking over large spatial scales and then as it proceeds downwards to the lower layers the speed criteria are refined until it arrives at the raw image pixels.

3 Methodology

In this section we describe the methodology followed for estimating a moving robot's speed relative to a fixed camera through principal point estimation and optical flow. For this purpose the focal length of the camera, f , is varied in order to exploit the apparent motion of the objects in the image plane. Figure 1 provides a pictorial representation of the optical axis and the principal point as well as the various focal lengths a zoom lens can have. In this figure, it can also be seen how the focal length, f , of the camera affects the field-of-view (FOV). This relationship is expressed by (6),

$$FOV = \tan^{-1} \frac{d}{2f} \quad (6)$$

where d is the sensor's width. In general, in our method we attempt to keep the number of assumptions to as few as possible while at the same time develop a system that is flexible and efficient. In particular, the visual sensor we have employed is a SONY TX-9 digital camera with 4x optical zoom. The camera is uncalibrated and is placed parallel to the ground and orthogonal to the direction of motion of the mobile robot, hence, the optical axis of the camera is perpendicular to the direction of motion of the vehicle. The geometrical parameters of the camera as well as the distance between the camera and the moving vehicle are unknown. In addition, the distance that the moving vehicle has covered from time frame F_{t_i} to time frame $F_{t_{i+1}}$ which is needed to perform the optical flow algorithm is unknown. The only known parameter in this method is the height of the camera from the ground.

3.1 Principal Point Estimation

First, we estimate the principal point using optical flow. The LK algorithm is applied to two frames taken from the same position and orientation. One frame is taken at a focal length of 4 mm and the other one at 5 mm. We then perform a combination of the *jackknife* sampling method along with the minimization of the set of linear equations¹. Every optical flow vector represents a linear equation and the minimization of the system yields the position, P , at which the optical flow vectors converge. Thus, a set Ω_i is formed for every optical flow vector. Equations (7) and (8) show an example of two vectors,

$$P \in \Omega_1 = \{h \in \mathbb{R}^2 \mid \underbrace{(v_1 - r_1)^T}_{\alpha_1} h = \underbrace{v_1^T \cdot r_1 - \|r_1\|^2}_{\beta_1}\} \quad (7)$$

$$P \in \Omega_2 = \{h \in \mathbb{R}^2 \mid \underbrace{(v_2 - r_2)^T}_{\alpha_2} h = \underbrace{v_2^T \cdot r_2 - \|r_2\|^2}_{\beta_2}\} \quad (8)$$

where r is the position of the vector, and v is a point on a line that is perpendicular to the optical flow vector. The following equations, (9) and (10), show the process for $n - 1$ of optical flow vectors. Noise in the system is represented by variable ϵ_i .

$$\begin{aligned} h\alpha_1 + \epsilon_1 &= \beta_1 \\ h\alpha_2 + \epsilon_2 &= \beta_2 \\ &\vdots \\ h\alpha_{n-1} + \epsilon_{n-1} &= \beta_{n-1} \end{aligned} \quad (9)$$

$$h \in \operatorname{argmin} \sum_{i=1}^{n-1} (h\alpha_i - \beta_i + \epsilon_i)^2 \quad (10)$$

¹ The non-parametric method we have developed for outlier removal aims at avoiding the known risks entailing the use of parametric methods, such as RANSAC.

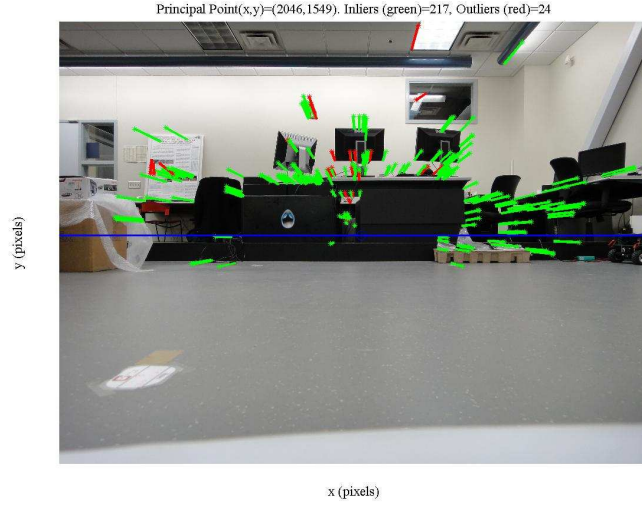


Fig. 2. Principal point estimation using optical flow. The outliers (red color) have been removed using the *jackknife* sampling method. The green color vectors denote inliers. The center of blue circle is the principal point that lies along the horizon line. Some profound outliers that have accurately been detected appear on the poster and on the window; x,y point is in Cartesian coordinates.

$$\underbrace{\left(\sum_{i=1}^{n-1} \alpha_i \alpha_i^T + \epsilon_i \right)}_C h = \underbrace{\left(\sum_{i=1}^{n-1} \alpha_i \beta_i \right)}_{\gamma} \quad (11)$$

$$h = C^{-1} \gamma \quad (12)$$

In (11) C is a 2×2 matrix and $\gamma \in \mathbb{R}^2$. The convergence point, P , is thus given by h . The *jackknife* sampling works by excluding one optical flow vector from the sample while estimating the point P using the $n - 1$ vectors of the data set. The Euclidean distance, $d(p_j, P_i)$, is then calculated between point p_j of the excluded vector and the convergence point, P_i . The same process is repeated n times, i.e., once for each optical flow vector within the given data set. The result is a set of n distances. The optical flow vectors whose distance is beyond the 90th percentile are considered as outliers and are disregarded. After outlier removal using *jackknife*, equations (9)-(12) are used to find the convergence point. Figure 2 depicts an image with the optical flow vectors used to estimate the principal point.

3.2 Speed Estimation

After having estimated the principal point the speed of the vehicle is calculated; this is achieved by means of optical flow, too. The principal point is used as a

reference point in the image in order to map heights to distances. The height is derived from the principal point on one end and the ground floor point, extracted from the motion of the robot, on the other end. The average time for the camera to acquire two continuous time frames has been estimated at $0.15s$. For this purpose we have used the *burst* mode of the digital camera. The well-known formula that describes the instantaneous speed, v , at time t is given by (13),

$$v(t) = \frac{\Delta s}{\Delta t} = \frac{ds}{dt} \quad (13)$$

where Δs is the distance covered in time interval Δt . Given the fact that our camera is placed parallel to the ground and the projection of the camera height onto the image plane is known, we estimate the distance traveled between the two time frames, D_r , using the cross ratio between the height of the camera from the ground in the image plane (in pixels), h_p , the real height of the camera from the ground (in *cm*), H_r , and the magnitude of optical flow vectors (in pixels), D_p , from the displacement of the vehicle within two time continuous frames. The following equation (14) describes this relationship

$$\frac{h_p}{H_r} = \frac{D_p}{D_r}. \quad (14)$$

From the previous equation it can be concluded that the distance Δs the moving vehicle has traveled in Δt is given by the variable D_r . Upon implementation of the LK algorithm on two continuous time frames, a set of optical flow vectors is generated with varying magnitudes and directions. Due to noise in sensor perception as well as due to factors such as occlusion, the optical flow vectors that appear on the moving object are not of equal magnitude. The vectors whose magnitude is below a given threshold are not considered as well as the vectors that fall outside of the tracked region, i.e., the region extracted from the difference of two images. Yet, after repeating a number of trials we have observed a number of vectors with small magnitudes. This is treated as noise due to the fact that robot motion yields optical flow vectors with significantly larger magnitudes. In order to calculate the instantaneous speed, the median value is selected from the distribution of the magnitudes of the vectors.

The magnitude of optical flow vectors in the x-direction is mapped to the height of the object in the image plane in order to convert from pixels to meters. This holds true since the height of the object does not change between the two frames. Moreover, the orientation of the optical axis of the camera being perpendicular to the direction of motion of the vehicle does not affect the height of the camera in the image plane due to perspective projection. In addition, estimating robot's speed on a ramp (Fig. 3) is as accurate as on a flat surface. This is due to the fact that optical flow vectors are parallel to the image plane.

In order to calculate the height of the vehicle in the image plane, we extract the object from its background using the difference between the time frames. We then threshold the image for the purpose of converting it into a binary one. The contour of the moving vehicle is extracted by applying a morphological operation to the image. In order to remove small objects from the binary image,

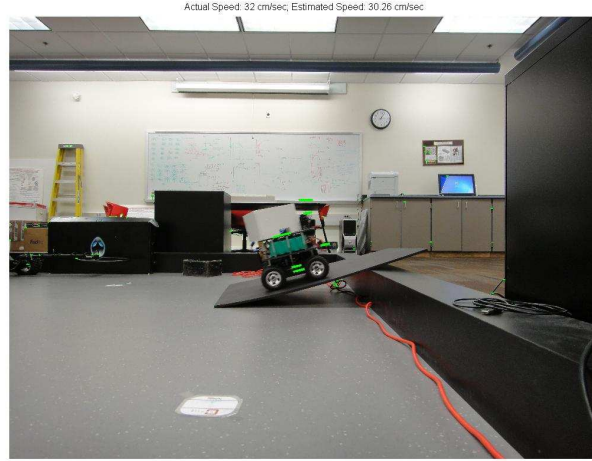


Fig. 3. Optical flow vectors at a ground truth speed of 32 cm/sec and $\simeq 15^\circ$ of angle. The estimated speed is 30.26 cm/sec.

all connected components that have fewer than δ pixels are removed. In our images the value of δ was set to 60 pixels. This was a result of trial and error. Figure 4 shows the result of the operation of absolute differences between two frames and the implementation of the morphological operation on the same image. The contour of the moving vehicle is required in order to find the height of the camera, that is, the distance between the principal point and the ground. Figure 5 depicts the contour of the robot in two time continuous images (green color), the principal point in blue circle, and the projection of camera height onto the image plane (red color). We have tested our algorithm with varying speeds as well as multiple times with the same speed.

4 Results

In this section we present the results from the methods we have employed to estimate the principal point and hence the speed of the mobile robot. One advantage of our approach for determining the speed of the robot is that it requires only two time continuous snapshots to be taken as we do not estimate the mean speed but rather the instantaneous speed of the vehicle. Table 1 summarizes the results between actual and estimated speed as well as the absolute and the relative error between actual and estimated speed. The actual speed of the robot was calculated by averaging the speed of 5 trials between two known points on the ground while keeping constant the motor command values for speed during each set of trial. The same process was repeated for all 8 different speed estimates. Interpreting the results of Table 1 the estimated speed is underestimated

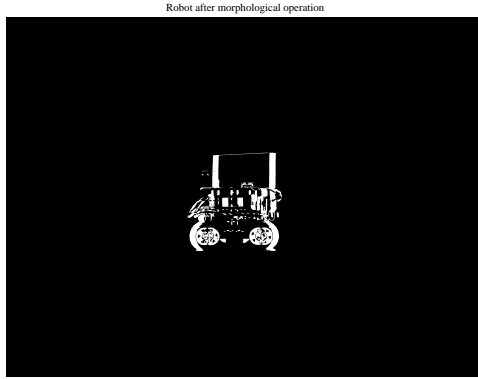


Fig. 4. Result of absolute differences between the two images used for speed estimation. Small objects have been removed using morphological operation on the image.

against the actual speed. The mechanism to correct this bias is through the use of linear regression.

Table 1. Speed Estimation Results

Actual Speed (<i>cm/sec</i>)	Est Speed	Abs Error	Rel Error (%)
14.5	13.18	1.32	9.1
21.92	19.84	2.08	9.49
30.38	27.74	2.64	8.69
35.89	33.76	2.13	5.93
41.91	37.49	4.42	10.55
48.62	42.88	5.74	11.81
53.52	50.04	3.48	6.5
58.27	52.83	5.44	9.34
32.0 ($\simeq 15^\circ$ angle)	30.26	1.74	5.44

Figure 6 shows the optical flow vectors at different robot speeds. Our results reveal that there is, on average, an error of approximately 3.4 cm/sec which is considered normal since parameters such as the extraction of the contour of the robot, the measured time between frames, or a small time drifts in measuring the actual speed can influence the estimated speed.

For principal point estimation the LK algorithm proved to be a rational approach. This is due to the fact that indoor environments provide an abundance of geometrical objects and hence corners and edges. The *jackknife* sampling method successfully identified the outliers in the images although discarding optical flow vectors whose distance is beyond the 90th percentile may lead to some inliers being treated as outliers. Nevertheless, this seems not to affect the final

Contour of robot between two frames (green square). Principal point (center of blue circle). Projection of camera height (red vertical line).

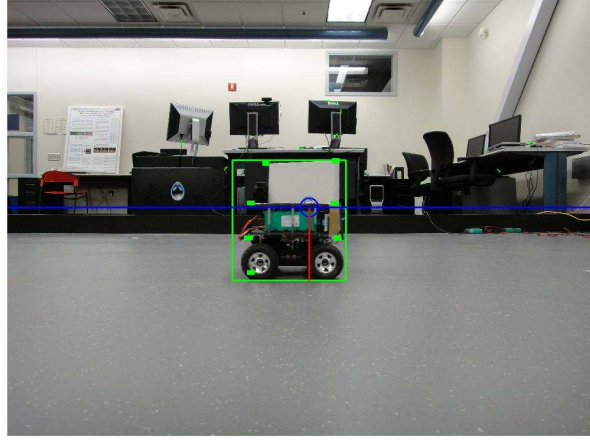


Fig. 5. Layout of the moving robot in two time continuous images (green rectangle). The blue circle depicts the principal point along the horizon line. The red vertical line is the projection of the camera height, H_r , from the ground to the principal point, onto the image plane (h_p). The magnitude of the green optical flow vectors depict the translation of robot between two images (D_p). The distance covered by the robot, D_r , is calculated from all the above (see also equation (14)).

outcome. The parameter that plays a significant role in estimating the principal point is the length of the focal points between the two successive images. We experimented with various focal lengths and we concluded that a large displacement between two focal lengths can influence significantly the estimation of the principal point. This has an immediate effect to the estimation of the speed of the robot.

For the estimation of the speed of the robot a critical parameter is the accurate extraction of the robot's layout, in particular with respect to the ground. This is required so as to map accurately the height of the camera on the image plane. In our method extracting the layout of the robot using morphological operators proved to be satisfactory. Nevertheless, for more complex environments a sophisticated algorithm will be needed. Yet, our method produced satisfactory results even when the snapshots of the robot were taken off the center of the image plane (Fig. 6).

5 Conclusions and Future Work

In this research we exploit the potential of optical flow to estimate both the principal point on an image as well as the speed of a mobile robot. Although speed estimation is a well-studied problem, we offer a new perspective to this problem by reducing the assumptions needed to one only known parameter,

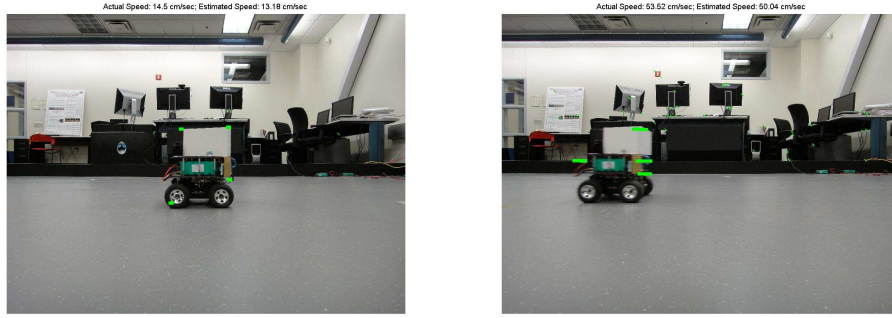


Fig. 6. Optical flow vectors at a ground truth speed of 14.5 cm/sec and 53.52 cm/sec (left to right). The estimated speed is 13.18 cm/sec and 50.04 cm/sec, respectively.

that is, the height of the camera from the ground. In spite of the fact that the grabbing of images was taken offline due to exclusively technical reasons (i.e., on one hand, we could not process the images while they were taken by the digital camera; on the other hand, plain webcams do not provide optical zoom), we firmly believe that our method has all the potentials to be implemented in real-time. Furthermore, there is no need for reference points in the image or the environment. This is relaxed by knowing the distance between the camera and the ground, an insignificant problem. In general, we have shown that our method proves to be parsimonious yet effective irrespective of the vehicle's speed, and the distance between the camera and the moving vehicle.

Our findings show that there is a more accurate estimation of the principal point when the focal length displacement of the camera between two images is increased by the smallest possible amount. In our experiments, this amount equals to 1 mm between the focal points of two given images. The larger the displacement, the higher the error in estimating the principal point and hence the speed of the vehicle. This also reveals that estimating the FOE may be hard since near (pure) translation using a mobile robot can be a difficult thing to attain.

The results of this research can be extended further in several ways. Our current research involves the estimation of a robot's own speed with respect to stationary objects. In addition, the acceleration can be estimated using the methods described. Since the vanishing point is surfing on the horizon in the case of a camera being parallel to the ground, this method can provide the means of estimating more accurately the vanishing point and the vanishing lines in an image plane, an important parameter for detecting roads among others [15]. Future work will consider the application of this method on an Unmanned Aerial Vehicle (UAV).

Acknowledgments. This research has been supported by the U.S. Office of Naval Research grant no. N000140911174 as part of the COMRADES project.

References

1. Indu, S., Gupta, M., Bhattacharyya, A.: Vehicle Tracking and Speed Estimation Using Optical Flow Method. *International Journal of Engineering Science and Technology*, vol. 3, no. 1, 429–434 (2011)
2. Dailey, D.J., Cathey, F.W., Pumrin, S.: An Algorithm to Estimate Mean Traffic Speed Using Uncalibrated Cameras. *IEEE Transactions on Intelligent Transportation Systems*, vol. 1, no. 2, 98–107, (2000)
3. Dogan, S., Temiz, M.S., Kulur, S.: Real Time Speed Estimation of Moving Vehicles from Side View Images from an Uncalibrated Video Camera. *Sensors*, vol. 10, no. 5, 4805–4824, (2010)
4. Honegger, D., Greisen, P., Meier, L., Tanskanen, P., Pollefeys, M.: Real-time Velocity Estimation Based on Optical Flow and Disparity Matching. In: *Proceedings of the IEEE/RSJ International Conference on Intelligent Robots and Systems*, pp. 5177–5182, (2012)
5. Grammatikopoulos, L., Karras, G., Petsa, E.: Automatic Estimation of Vehicle Speed From Uncalibrated Video Sequences. In: *Proceedings of the International Symposium on Modern Technologies, Education and Professional Practice in Geodesy and related Fields*, pp. 332–338, (2005)
6. Muller, J., Paul, O., Burgard, W.: Probabilistic Velocity Estimation for Autonomous Miniature Airships using Thermal Air Flow Sensors. In: *Proceedings of the International Conference on Robotics and Automation*, pp. 39–44, (2012)
7. Bauer, D., Belbachir, A.N., Donath, N., Gritsch, G., Kohn, B., Litzenberger, M., Posch, C., Schon, P., Schraml, S.: Embedded Vehicle Speed Estimation System Using an Asynchronous Temporal Contrast Vision Sensor. *EURASIP Journal on Embedded Systems*, vol. 2007, no. 1, 1–12, (2007)
8. Kassem, N., Kosba, A.E., Youssef, M.: RF-based Vehicle Detection and Speed Estimation. In: *Proceedings of the 75th IEEE Vehicular Technology Conference*, pp. 1–5 (2012)
9. Ernst, J.M., Ndoye, M., Krogmeier, J.V., Bullock, D.M.: Maximum-Likelihood Speed Estimation using Vehicle-Induced Magnetic Signatures. In: *IEEE International Conference on Intelligent Transportation Systems*, pp. 1–6, (2009)
10. Chen, Z., Pears, N., Liang, B.: A Method of Visual Metrology From Uncalibrated Images. *Pattern Recognition Letters*, vol. 27, no. 13, 1447–1456, (2006)
11. Criminisi, A., Reid, I., Zisserman, A.: Single View Metrology. *International Journal of Computer Vision*, vol. 40, no. 2, 123–148, (2000)
12. Momeni-K., M., Diamantas, S.C., Ruggiero, F., Siciliano, B.: Height Estimation From a Single Camera View. In: *Proceedings of the International Conference on Computer Vision Theory and Applications*, pp. 358–364. *SciTePress* (2012)
13. Fayman, J.A., Sudarsky, O., Rivlin, E., Rudzsky, M.: Zoom Tracking and its Applications. *Machine Vision and Applications*, vol. 13, no. 1, 25–37, (2001)
14. Lucas, B.D., Kanade, T.: An Iterative Image Registration Technique with an Application to Stereo Vision. In: *Proceedings of the 7th International Joint Conference on Artificial Intelligence*, pp. 674–679, (1981)
15. Kong H., Audibert, J.-Y., Ponce, J.: Vanishing Point Detection for Road Detection. In: *IEEE Conference on Computer Vision and Pattern Recognition*, pp. 96–103, (2009)